*Progress In Electromagnetics Research Letters, Vol. 107, 67–74, 2022*

# A Low-Profile and Low-Cost Dual Circularly Polarized Patch Antenna

**Zahra Mousavirazi[1, *], Hassan Naseri[1], Mohamed Mamdouh M. Ali[2], Pejman Rezaei[3], and Tayeb A. Denidni[1]**

**Abstract**—This paper presents a low profile and low-cost patch antenna with dual circularly polarized (CP) capability in X-band at a canter frequency of 8.3 GHz. The dual-CP antenna is divided into three layers, composed of a parasitic square patch, a radiation square patch with four equal arms, and a 90° patch coupler. Two arms of the radiation patch are connected to the 90° hybrid coupler using two metalized vias. Right-handed circular polarization (RHCP) and left-handed circular polarization (LHCP) are achieved by exciting two different ports. To validate the proposed design, the prototype of the dual-CP antenna is fabricated and measured. Based on the measurement, the structure of the proposed antenna has an excellent circular-polarization purity of less than 3 dB over the whole operational frequency bandwidth of the antenna (8 GHz–8.47 GHz) with a wide 3-dB axial ratio (AR) beamwidth of 133° across the angular range from −55° to +78° at 8.3 GHz.

## 1. INTRODUCTION

With the rapid development of modern communication systems, the demand for compact and low-cost dual circularly polarized (CP) antennas has attracted immense attention due to their capabilities of increasing the capacity of wireless communication, reducing multipath interference, and requiring no strict orientation between receiving and transmitting antennas [1–5]. One of the alternative approaches to produce circular polarization is to create two orthogonal resonant modes on the radiating element with a 90° phase difference. CP patch antennas are usually categorized into two classes, 1) single-feed [6] and 2) dual-feed classes [7, 8]. Single-feed categories are simpler but generally suffer from a limited Axial Ratio (AR) bandwidth. On the other hand, the dual-feed solution results in a larger AR bandwidth at the expense of a more intricate feeding network. Both these configurations can excite orthogonal principal modes of the patch with a 90° phase shift and allow the use of either right-handed circular polarization (RHCP) or left-handed circular polarization (LHCP), but not simultaneously [9].

In [10–12], several structures, providing circular polarization diversity, have been reported. Nevertheless, these antennas can only realize a single CP mode (LHCP or RHCP). In [13], a dual-CP patch antenna fed by a multimode coplanar waveguide (CPW) transmission line has been proposed, but each CP is generated in different frequency bands. A good solution to have dual CP in a specific frequency band is to use a hybrid coupler as a dual-fed microstrip patch antenna [14, 15]. The coupler provides the 90° phase shift needed for CP, and the antenna radiates either LHCP or RHCP, depending on the excited port [16, 17]. A dual-feed CP microstrip antenna fed by a reconfigurable hybrid coupler 90° has been demonstrated in [18] which suffers from narrow impedance and AR bandwidth. Recently, in [19] a crescent-shaped slot antenna with the capability of producing dual-CP is introduced, but the proposed structure radiates in two directions which is not useful for unidirectional applications. The main purpose

*Received 6 July 2022, Accepted 10 October 2022, Scheduled 25 October 2022*

* Corresponding author: Zahra Mousavirazi (zahra.mousavirazi@inrs.ca).

[1] National Institute of Scientific Research (INRS), Montreal (QC), Canada. [2] Department of Electrical Engineering, Faculty of Engineering, Assiut University, Assiut, Egypt. [3] Electrical and Computer Engineering Faculty, Semnan University, Semnan, Iran.

of the proposed antenna is to design a compact dual-CP antenna with wide AR beamwidth. The antenna provides both left-handed circular polarization (LHCP) and right-handed circular polarization (RHCP) by choosing port 1 or port 2. For a CP antenna, 3 dB axial-ratio beamwidth (ARBW) is an important index that describes the performance of signal coverage. For example, geostationary satellite receiver antennas used at high latitudes must have a wide ARBW. Furthermore, an important fact is that the above-mentioned antennas suffer from a low AR beamwidth. So, it is required to design a compact and low-profile dual-CP structure with a good impedance bandwidth, 3-dB AR bandwidth, and beamwidth.

In this paper, a dual-CP patch antenna using a 90° hybrid patch coupler and compact structure for X-band applications at 8.3 GHz is proposed. The X-band antenna beam is required to be circularly polarized and has a wide AR beamwidth. The proposed antenna can generate either RHCP or LHCP broadside radiation patterns by exciting different ports with great isolation between RH- and LH-polarizations over 15 dB. Moreover, this antenna has the advantages of easy processing, low cost, light weight, and good CP performance. Good agreement between simulated and measured results is obtained.

## 2. DUAL-CP ANTENNA DESIGN AND PERFORMANCE

Figure 1 illustrates the configuration of a dual-CP patch antenna fed by a 90° coupler. The compact dual-CP antenna consists of three dielectric layers with the same thickness of 0.508 mm, and all three layers are Rogers RO4003 substrates with the dielectric constant of $\varepsilon_r = 3.55$ and loss tangent of $\tan\delta = 0.0027$. The feed network is located at the bottom side of the first substrate, which is made of two feed arms and a square patch having a cross-shaped slot with unequal widths. A ground surface isolates the first layer from the second. A radiation square metal patch with four rectangular-shaped arms is located between the second and third layers, which is connected to the feed network using two metalized vias. A parasitic metallic-square-patch as shown in Fig. 1(e) with width $L_3 = 8.2$ mm is also embedded at the upper side of the third layer to improve the antenna gain.

### 2.1. Design of the 90° Coupler

The geometry of the proposed 90° rectangular patch coupler with two rectangular slots with different widths ($d_1$ & $d_2$) is shown in Fig. 1(b). The importance of the 90° couplers is concealed in two main roles: 1) produce a 90-degree phase shifting at output ports, 2) divide input power into two equal parts. The slots in the patch prevent returned signal into input port 2 and divide the signal into two equals for output ports (ports 3 & 4), and also they cause the creation of 90° phase shift at output ports.

The simulated results of the designed 90° coupler are depicted in Fig. 2. The coupler provides a $90° \pm 5°$ phase difference ($\angle S_{13}$–$\angle S_{14}$) between output ports over the operating bandwidth from 7.8 to 8.8 GHz and $-4 \pm 0.5$ dB bandwidth between 6.56 GHz and 8.45 GHz. Moreover, using the coupler in the input ports of the antenna leads to large isolation between its two input ports. The full-wave simulator CST Microwave Studio is used to simulate and optimize the proposed single antenna.

### 2.2. Performance of the Antenna

The hybrid coupler placed on the bottom of the first substrate is excited via one of its input ports, and subsequently, the input signal is divided into two similar signals with a 90-degree phase difference. The metalized vias transfer the signals to the arms of the patch antenna. It is also worth mentioning that the ground does not let any unwanted signal disturb the performance of the radiating patch. As a result of the fact that the patch is fed from its two adjacent edges, the orthogonal resonant modes are excited, and a 90-degree phase difference provided by the coupler brings about a radiation pattern with circular polarization. Exciting the other input port of the coupler can produce the same radiation pattern as the other mode of CP (left- or right-handed mode).

When it comes to talking about the parasitic patch placed on top of the third substrate, it should be clarified that it radiates at a frequency so close to the resonant frequency of the main patch (patch on the second substrate), and consequently, the gain of the antenna improves. The simulated results of the gain variation in terms of loading the patch are shown in Fig. 3. It can be seen that the CP antenna gain is improved by up to 2 dBi using the parasitic patch. It is also worth mentioning that the presence

of the parasitic patch has no destructive effect on the reflection coefficient and AR bandwidth of the CP antenna.

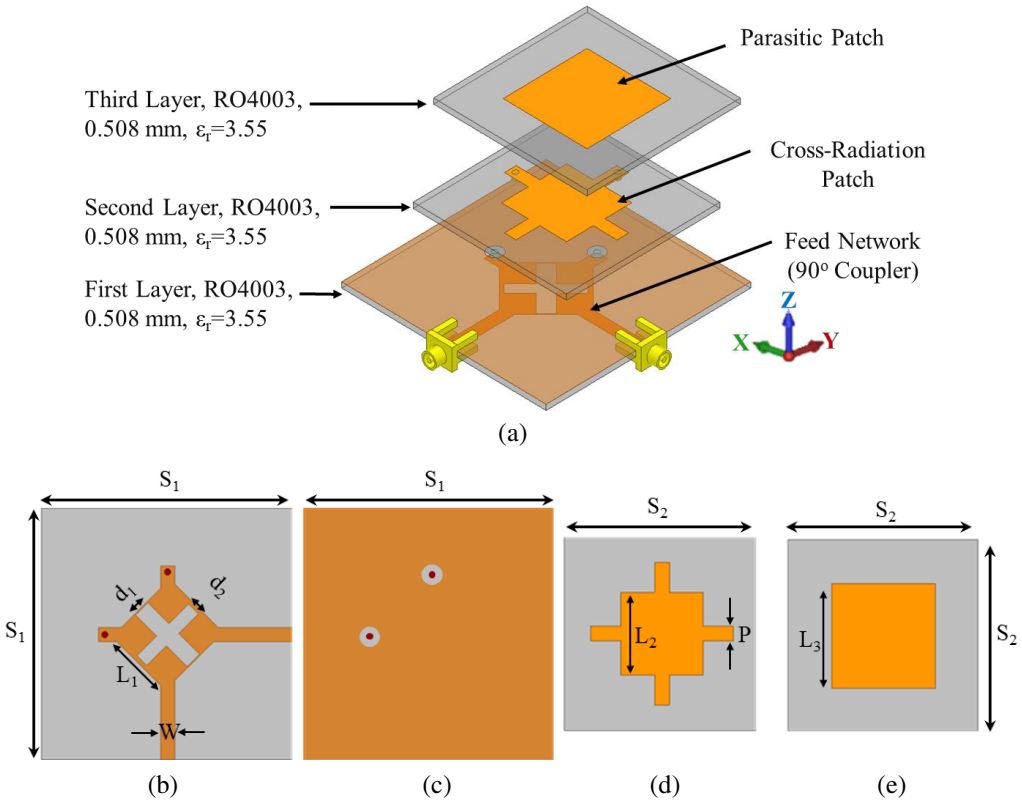


**Figure 1.** Geometry of the proposed dual-CP antenna: (a) 3-D view, (b) the feed network structure (bottom view); (c) top view of the feed network; (d) top view of the cross-radiation patch; and (e) top view of the parasitic patch. (Design parameters (all in millimetres): $S_1 = 23$, $d_1 = 1.4$, $d_2 = 1.1$, $L_1 = 4.38$, $W = P = 1.14$, $L_2 = 6.36$, $L_3 = 8.2$, and $S_2 = 15$.

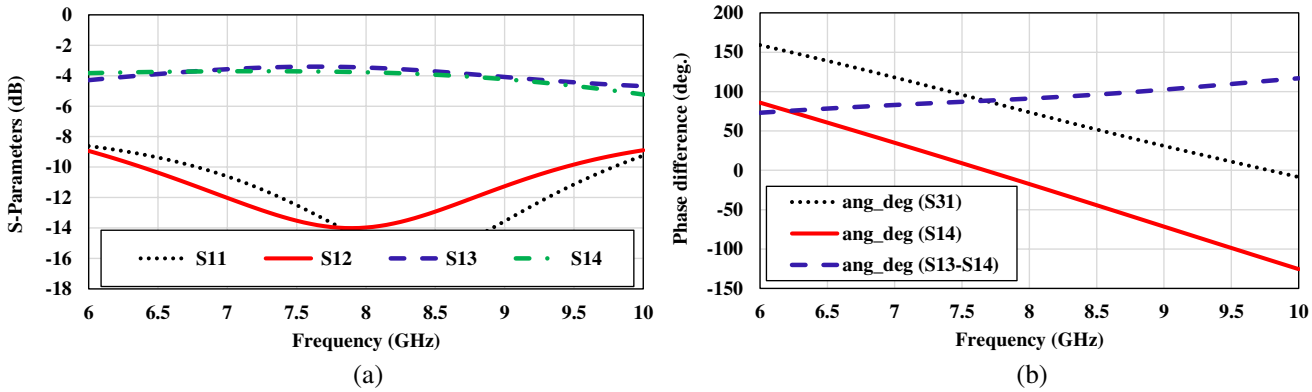


**Figure 2.** Simulated results of the designed 90° coupler: (a) $S$-parameters response; and (b) phase difference adjacent output ports for port 1.

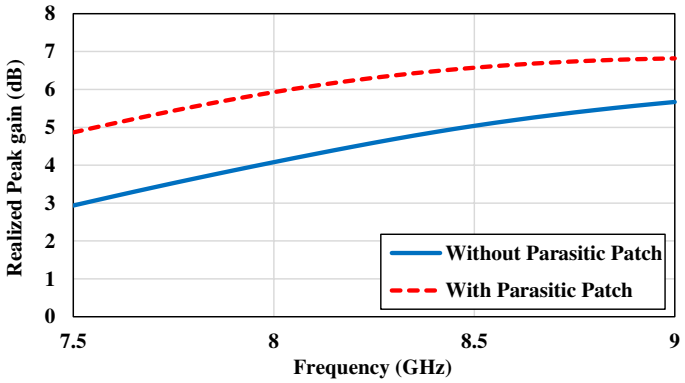


**Figure 3.** Simulated realized peak gain of the proposed CP antenna with and without the parasitic square patch.

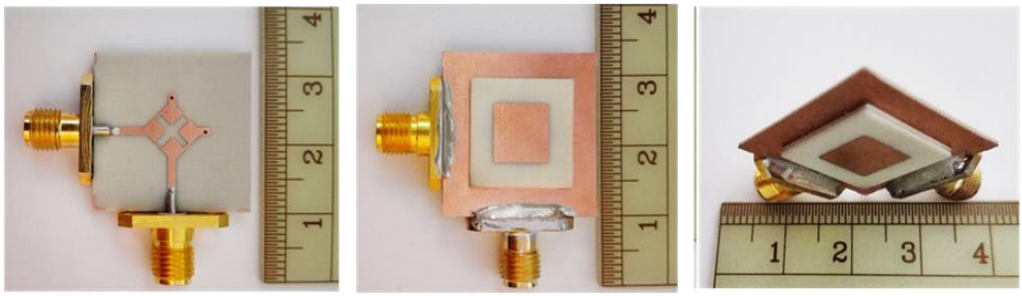

(a) (b) (c)

**Figure 4.** Photography of the fabricated dual-CP antenna; (a) bottom view; (b) top view; and (c) 3D view.

## 3. EXPERIMENTAL VERIFICATION AND DISCUSSION

A dual-CP antenna was fabricated and measured to validate the proposed structure as shown in Fig. 4. The fabrication process can be simply described as follows. First, all the layers (The parasitic patch layer, cross radiation patch layer, and feeding network layer) of the structure are fabricated separately and then fixed together under pressure with glue. The scattering parameters are measured by R&S® ZNB Vector Network Analyzer. The measurements of the radiation pattern are done in a compact anechoic chamber. A horn antenna is used as a transmitter at the focal point of the reflector to convert the spherical to plane waves toward the antenna under test (AUT) in the receive mode, as shown in Fig. 5. The AR is measured using an anechoic chamber, whose two measurements were performed with the help of the standard dipole antenna in 0° orientation angle (for $E_\theta$) and 90° orientation angle (for $E_\phi$). Then, using the phase-amplitude method as the following equations, the ERHCP, ELHCP, and AR are calculated [20, 21]:

$$E_{RHCP} = \frac{1}{\sqrt{2}}\left(E_\theta + E_\varphi\right) \tag{1}$$

$$E_{LHCP} = \frac{1}{\sqrt{2}}\left(E_\theta - E_\varphi\right) \tag{2}$$

$$AR = -\frac{\left(|E_{RHCP}| + |E_{LHCP}|\right)}{\left(|E_{RHCP}| - |E_{LHCP}|\right)} \tag{3}$$

The simulated and measured scattering parameters of the single dual-CP antenna are plotted in Fig. 6. The measured result shows that the proposed antenna provides an impedance bandwidth

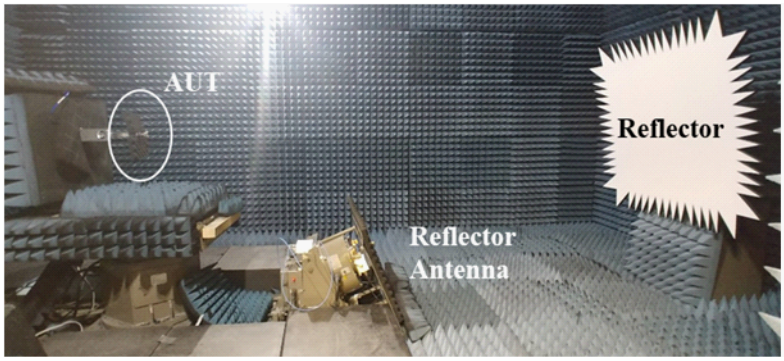


**Figure 5.** Radiation pattern measurement setup.

($S_{11} \leq -10$ dB) of 8.15% from 8.12 to 8.81 GHz with isolation better than 12 dB over the whole frequency bandwidth. Fig. 7 shows the simulated and measured radiation patterns of the dual-CP prototype at 8.3 GHz. Two distinct input ports provide both RHCP and LHCP radiations. When Port 1 is excited, an RHCP beam is obtained, and when Port 2 is excited, an LHCP beam is generated. It is obvious that the main beam of the antenna array is successfully radiated in two different polarizations with isolation between RH and LHCP over 15 dB. The simulated and measured gains and ARs versus frequency are displayed in Fig. 8. The measured AR is less than 3-dB in the frequency bandwidth from 8 to 8.47 GHz in the broadside direction ($\theta = 0°$) with the realized peak gain of 6.19 dB at 8.3 GHz. A wide ARBW of 133° is obtained from $-55°$ to $+78°$ with the AR remaining below 3-dB, which means that a pure CP is achieved in the wide broadside $\theta$ bandwidth as indicated in Fig. 9.

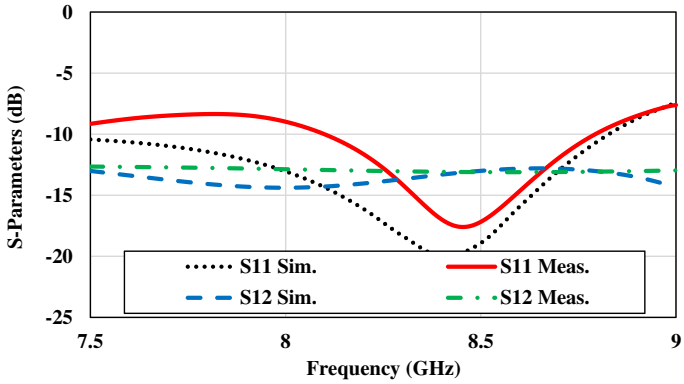


**Figure 6.** Simulated and measured $S$-parameters of the proposed dual-CP single antenna.

## 4. COMPARISON WITH RECENTLY PUBLISHED DUAL-CP ANTENNAS

A brief comparison between the results and performance of the proposed antenna with some recently published dual-CP antennas is shown in Table 1. As it is evident, one of the important parameters not mentioned and taken into consideration in previous works [18, 19] is related to AR beamwidth which is good in this work. Also, the pattern configuration in [19] cannot be useful when one wants to utilize it in unidirectional applications. Furthermore, the realized gain in this work is better than [19]. Most of the CP antennas with wide AR beamwidth presented in the literature have a narrow impedance bandwidth [22–24] with a single polarization mode. The proposed CP antenna can provide not only dual CP polarizations but also wide AR beamwidth. Although this design has the narrowest impedance and AR bandwidths due to its smallest size, the obtained results are sufficient to cover the targeted

application. It should be mentioned that by choosing another parasitic patch, it is possible to improve the impedance bandwidth of the structure or even make it a dual-band. Thus, it indicates the flexibility of the proposed antenna. The results are indicative of the fact that the dual CP antenna suggested in this paper has better performance than similar previous published works.

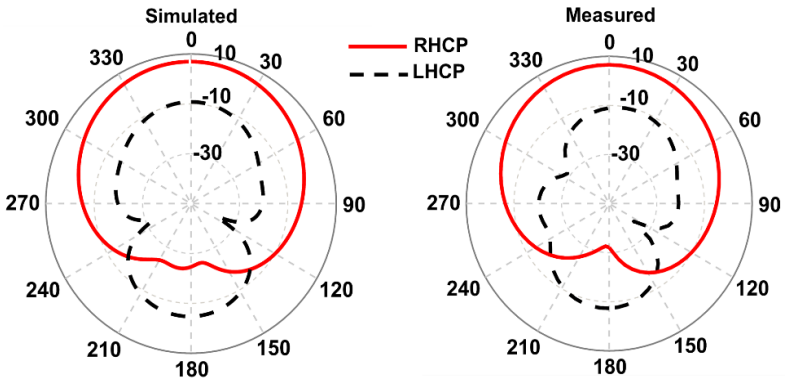


(a) Port 1

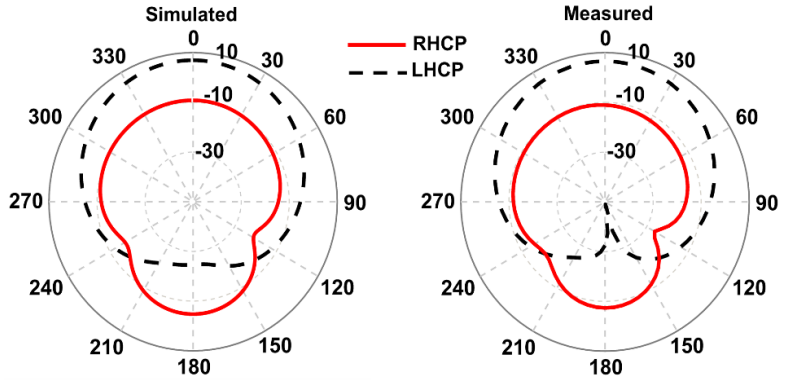


(b) Port 2

**Figure 7.** Simulated and measured radiation patterns of the single antenna for each input port at 8.3 GHz: (a) Port 1; (b) Port 2.

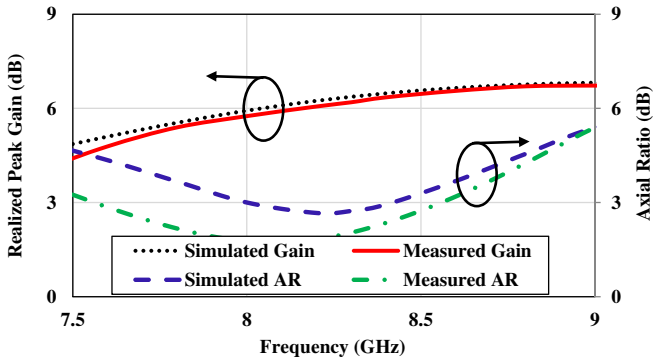


**Figure 8.** Simulated realized peak gain and AR versus frequency of the designed dual-CP antenna port 1.

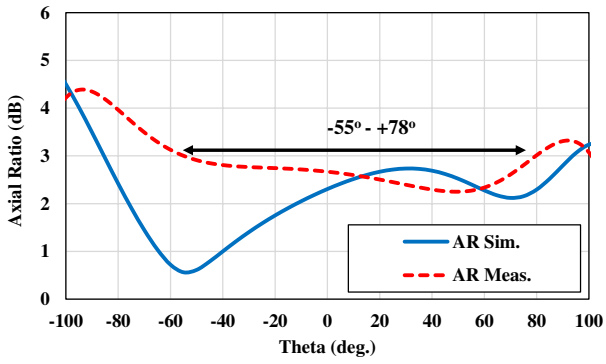


**Figure 9.** Simulated and measured AR versus theta of the proposed dual-CP antenna at 8.3 GHz.

**Table 1.** Comparison between this work and previous counterparts.

| Ref. | Freq. (GHz) | Impedance Bandwidth | AR Bandwidth | Pattern Configuration | Gain (dBi) | AR beamwidth | Polarization Type |
|---|---|---|---|---|---|---|---|
| [18] | 5.4 | 2% | NA | Omnidirectional | 6.5 | NA | Dual CP (RH/LH CP) |
| [19] | 3.5 | 33% | 33% | Bidirectional | 5 | NA | Dual CP (RH/LH CP) |
| [22] | 5.8 | 3.97% | 4% | Omnidirectional | 0.92 | 60° (−30 to +30) | LHCP |
| [23] | 2.28 | 1.56% | 0.88% | Unidirectional | 7 | 120° (−60 to +60) | LHCP |
| [24] | 1.57 | 2.4% | 0.6% | Omnidirectional | 7.9 | 138° (−75 to +63) | RHCP |
| This work | 8.3 | 8% | 5% | Unidirectional | 6.19 | 133° (−55 to +78) | Dual CP (RH/LH CP) |

## 5. CONCLUSION

A design of a dual-CP antenna has been studied and demonstrated at an 8.3 GHz ITU band. The proposed dual-CP antenna can generate reconfigurable LHCP or RHCP radiations by easily switching the two input ports. The simulated and measured results have shown that the dual-CP antenna has a pure CP radiation with AR maintained below 3-dB at the wide scan range of 133° obtained from −55° to +78°. This simple and compact antenna can be used for wireless communication applications such as mobile phones and Internet of Things (IoT) applications.

## REFERENCES

1. Yang, Y., B. Sun, and J. Guo, "A low-cost, single-layer, dual circularly polarized," *IEEE Antennas Wirel. Propag. Lett.*, Vol. 18, No. 4, 651–655, 2019.
2. Li, H. D., X. Y. Du, J. Y. Yin, J. Ren, and Y. Yin, "Differentially fed dual-circularly polarized antenna with slow wave delay lines," *IEEE Trans. Antennas Propag.*, Vol. 68, No. 5, 4066–4071, 2020.
3. Mousavi, Z., P. Rezaei, and V. Rafii, "Single layer CPSSA array with change polarization diversity in broadband application," *Int. J. RF Microwave Computer-Aided Eng.*, Vol. 27, No. 4, e21075, 2017.
4. Wu, Z., M. C. Tang, T. Shi, and R. W. Ziolkowski, "Two-port, dual-circularly polarized, low-profile broadside-radiating electrically small huygens dipole antenna," *IEEE Trans. Antennas Propag.*, Vol. 69, No. 1, 514–519, 2021.
5. Sun, M., Z. Zhang, K. An, X. Wang, Y. Jiang, and A. Chen, "Dual-sense circular polarization antenna based on reconfigurable orthogonal network," *Int. J. Antennas Propag.*, Vol. 2019, Article ID 1670786, 2019.
6. Sharma, P. and K. Gupta, "Analysis and optimized design of single feed circularly polarized microstrip antennas," *IEEE Trans. Antennas Propag.*, Vol. 31, No. 6, 949–955, 1983.
7. Adrian, A. and D. H. Schaubert, "Dual aperture-coupled microstrip antenna for dual or circular polarisation," *Electron. Lett.*, Vol. 23, No. 23, 1226–1228, 1987.

8. Mousavi, Z. and P. Rezaei, "Millimetre-wave beam-steering array antenna by emphasising on improvement of Butler matrix features," *IET Microwaves, Antennas & Propagation*, Vol. 13, No. 9, 1287–1292, 2019.
9. Caso, R., A. Buffi, M. R. Pino, P. Nepa, and G. Manara, "An annular-slot coupling feeding technique for dual-feed circularly polarized patch arrays," *2010 IEEE Antennas and Propagation Society International Symposium*, 1–4, Toronto, 2010.
10. Ali, M. M. M. and A. Sebak, "Printed RGW circularly polarized differential feeding antenna array for 5G communications," *IEEE Trans. Antennas Propag.*, Vol. 67, No. 5, 3151–3160, 2019.
11. Ding, K., C. Gao, T. Yu, D. Qu, and B. Zhang, "Gain-improved broadband circularly polarized antenna array with parasitic patches," *IEEE Antennas Wirel. Propag. Lett.*, Vol. 16, 1468–1471, 2017.
12. Xu, H., J. Zhou, K. Zhou, Q. Wu, Z. Yu, and W. Hong, "Planar wideband circularly polarized cavity-backed stacked patch antenna array for millimeter-wave applications," *IEEE Trans. Antennas Propag.*, Vol. 66, No. 10, 5170–5179, 2018.
13. Midya, M., S. Bhattacharjee, S. C. Bakshi, and M. Mitra, "CPW-fed dual-band dual-sence circularly polarized square slot antenna," *2018 IEEE Indian Conf. Antennas Propagation*, 4–6, 2018.
14. Mousavi, Z., P. Rezaei, M. B. Kakhki, and T. A. Denidni, "Beam-steering antenna array based on a butler matrix feed network with CP capability for satellite application," *Journal of Instrumentation*, Vol. 14, P07005-1–P07005-9, 2019.
15. Narbudowicz, A., X. Bao, and M. J. Ammann, "Dual circularly-polarized patch antenna using even and odd feed-line modes," *IEEE Trans. Antennas Propag.*, Vol. 61, No. 9, 4828–4831, 2013.
16. Mousavi, Z. and P. Rezaei, "A two-layer beam-steering array antenna with $4 \times 4$ modified Butler matrix fed network for switched beam application," *Int. J. RF Microwave Computer-Aided Eng.*, Vol. 30, No. 2, e22028, 2020.
17. Wang, A., X. Li, X. J. Yi, L. Yang, J. Zhao, and A. Li, "Dual circularly polarised omnidirectional antenna," *IET Microw. Antennas Propag.*, Vol. 13, No. 6, 870–873, 2019.
18. Moubadir, M., I. Badaoui, N. A. Touhami, M. Aghoutane, and M. El Ouahabi, "A new circular polarization dual feed microstrip square patch antenna using branch coupler feeds for WLAN/HIPERLAN applications," *Procedia Manuf.*, Vol. 32, 702–709, 2019.
19. Parchin, N. O., H. J. Basherlou, and R. A. Abd-Alhameed, "Dual circularly polarized crescent-shaped slot antenna for 5G front-end systems," *Progress In Electromagnetics Research Letters*, Vol. 91, 41–48, 2020.
20. Fakharian, M., P. Rezaei, and A. Orouji, "Reconfigurable multiband extended U-slot antenna with switchable polarization for wireless applications," *IEEE Antennas Propag. Mag.*, Vol. 57, No. 2, 194–202, 2015, doi: 10.1109/MAP.2015.2414665.
21. Mousavirazi, Z., V. Rafiei, and T. A. Denidni, "Beam-switching antenna array with dual-circular-polarized operation for WiMAX applications," *AEU — Int. J. Electron. C.*, Vol. 137, 153796, 2021, doi: https://doi.org/10.1016/j.aeue.2021.153796.
22. Chu, Q., M. Ye, and X. Li, "A low-profile omnidirectional circularly polarized antenna using planar sector-shaped endfire elements," *IEEE Trans. Antennas Propag.*, Vol. 65, No. 5, 2240–2247, 2017.
23. Liu, N.-W., L. Zhu, and W.-W. Choi, "Low-profile wide-beamwidth circularly-polarised patch antenna on a suspended substrate," *IET Microw. Antennas Propag.*, Vol. 10, No. 8, 885–890, May 2016.
24. Zhang, X., L. Zhu, N. W. Liu, and D. P. Xie, "Pin-loaded circularlypolarised patch antenna with sharpened gain roll-off rate and widened 3-dB axial ratio beamwidth," *IET Microw. Antennas Propag.*, Vol. 12, No. 8, 1247–1254, Mar. 2018.